

# Toward extracting scattering phase shift from integrated correlation functions III: coupled-channels

Peng Guo\*

*College of Arts and Sciences, Dakota State University, Madison, SD 57042, USA and  
Kavli Institute for Theoretical Physics, University of California, Santa Barbara, CA 93106, USA*

Frank X. Lee†

*Department of Physics, George Washington University, Washington, DC 20052, USA*

(Dated: December 3, 2024)

The formalism developed in Refs.[1, 2] that connects integrated correlation function of a trapped two-particle system to infinite volume scattering phase shift is further extended to coupled-channel systems in the present work. Using a trapped non-relativistic two-channel system as an example, a new relation is derived that retains the same structure as in the single channel, and has explicit dependence on the phase shifts in both channels but not on the inelasticity. The relation is illustrated by a exactly solvable coupled-channel quantum mechanical model with contact interactions. It is further validated by path integral Monte Carlo simulation of a quasi-one-dimensional model that can admit general interaction potentials. In all cases, we found rapid convergence to the infinite volume limit as the trap size is increased, even at short times, making it potentially a good candidate to overcome signal-to-noise issues in Monte Carlo applications.

## I. INTRODUCTION

Scattering is a ubiquitous tool in probing the nature of interactions between particles, either in atomic and molecular physics or in nuclear and particle physics. An effective theoretical approach is the use of a finite box with periodic boundary conditions to enclose the system under consideration. General relations can be established that connect the quantized energies of the system to the infinite-volume scattering phaseshifts, regardless of how the energy spectrum is obtained. The most famous of the approach is the Lüscher formula [3] which has been widely applied in the field of lattice QCD to obtain scattering parameters in hadron-hadron interactions [4–45]. In the case of nucleon-nucleon scattering, in addition to the Lüscher method, there is the potential method by the HALQCD collaboration [46–50] also relying on the discrete energy spectrum.

The nucleon-nucleon system presents unique challenges to such methods. First, the signal-to-noise (S/N) issue [51, 52] requires exponentially more statistics in stochastic evaluation of the path integral of the two-nucleon correlation. Second, at larger volumes the condensed energy spectrum requires a large number of interpolating operators to resolve [53]. The required Euclidean time to display the signal of clear plateau could be well into the region where the signal is swamped by noise. The challenges resulted in the so-called “two-nucleon controversy”: The results from the Lüscher formula method and HAL QCD potential method do not agree [52]. The issue is most likely in the energy spectrum extraction [54].

These challenges motivated alternative approaches in recent years. One is the spectral function based methods that utilize Bayesian inference [53, 55, 56]. Another is the integrated correlation function method proposed in Refs. [1, 2]. We showed that in a two-particle system, the difference between interacting and non-interacting integrated correlation functions in finite volume can be related to infinite-volume phase shift through a weighted integral. It is demonstrated that the relation has a rapid convergence rate at short Euclidean times, even with a modestly small sized box. The fast convergence at short Euclidean time makes it potentially a good candidate to overcome the S/N problem in two-nucleon systems. Since the formalism involves correlation functions rather than energy spectrum, it is in principle free from issues encountered at large volumes, such as increasingly dense energy spectrum and the extraction of low-lying states.

The aim of the present work is to extend the single-channel formalism in Refs. [1, 2] to beyond the elastic scattering region to include the effect of inelastic coupled-channel dynamics. We will limit our discussion to two-particle systems in two coupled channels with non-relativistic dynamics in one spatial dimension and one temporal dimension. Such a system can showcase the main ideas of the formalism while being amenable to testing by exactly solvable models. We also carry out Monte Carlo simulations to validate the new relation for coupled channels.

The paper is organized as follows. The single-channel integrated correlation function formalism is outlined briefly in Sec. II. The extension to coupled-channel systems is presented in Sec. III. A quasi-one-dimensional Monte Carlo test is presented in Sec. IV. Summary and outlook are given in Sec. V. Some technical details are in an appendix.

---

\* peng.guo@dsu.edu

† fxlee@gwu.edu

## II. SUMMARY OF SINGLE-CHANNEL INTEGRATED CORRELATION FUNCTION FORMALISM

In this section, we outline the basic ingredients needed for an extension of the formalism from single channel to two coupled channels.

In Ref. [1, 2], we derived a relation that connects the integrated correlation functions for two particles in a trap to the scattering phase shift,  $\delta(\epsilon)$ , through a weighted integral,

$$C(t) - C_0(t) \xrightarrow{\text{trap} \rightarrow \infty} \frac{it}{\pi} \int_0^\infty d\epsilon \delta(\epsilon) e^{-i\epsilon t}, \quad (1)$$

where  $C(t)$  and  $C_0(t)$  are integrated correlation functions for two interacting and non-interacting particles in the trap. The relation is derived in Minkowski time. Its Euclidean time version can be obtained by an analytical continuation ( $t \rightarrow -i\tau$ ),

$$C(\tau) - C_0(\tau) \xrightarrow{\text{trap} \rightarrow \infty} \frac{\tau}{\pi} \int_0^\infty d\epsilon \delta(\epsilon) e^{-\epsilon\tau}. \quad (2)$$

The integrated two-particle correlation function for non-relativistic systems is defined through summing over all the modes of two-particle correlation functions along the diagonal,

$$C(t) = \int dr C(rt; r0), \quad (3)$$

where  $C(rt; r'0)$  is the expectation value of time-ordered two-particle interpolating operators,

$$C(rt; r'0) = \langle 0 | \mathcal{T} \left[ \widehat{\mathcal{O}}(r, t) \widehat{\mathcal{O}}^\dagger(r', 0) \right] | 0 \rangle. \quad (4)$$

The  $\widehat{\mathcal{O}}^\dagger(r', 0)$  and  $\widehat{\mathcal{O}}(r, t)$  denote creation and annihilation operators to create two particles with relative coordinate of  $r'$  at time  $0$  at source, and then annihilate them with relative coordinate of  $r$  at time  $t$  at sink, respectively. See Refs. [1, 2] for more examples and technical details in both non-relativistic and relativistic systems.

On the other hand, two-particle correlation functions can be expressed in terms of wavefunctions in the spectral representation. For example, the forward time propagating non-relativistic two-particle correlation function is given by [1],

$$C(rt; r'0)|_{t>0} = \sum_\epsilon \psi_\epsilon(r) \psi_\epsilon^*(r') e^{-i\epsilon t}, \quad (5)$$

where the two-particle relative wavefunction for trapped systems satisfies the Schrödinger equation,

$$\left[ -\frac{1}{2\mu} \frac{d^2}{dr^2} + U_{\text{trap}}(r) + V(r) \right] \psi_\epsilon(r) = \epsilon \psi_\epsilon(r). \quad (6)$$

We use a unit system with  $\hbar = c = 1$ . The  $\mu$  denotes the reduced mass of the two-particle system,  $U_{\text{trap}}(r)$  trap

potential, and  $V(r)$  two-particle interaction potential. In this representation, the integrated version of Eq.(5) is simply related to the energy spectrum by,

$$C(t) = \sum_\epsilon e^{-i\epsilon t}. \quad (7)$$

The energy spectrum of trapped interacting systems can be determined by Lüscher formula-like quantization conditions, see e.g. discussions in Ref. [1, 2].

To connect the integrated two-particle correlation function to scattering phase shift in infinite volume, we use its Green's function representation [1, 2],

$$C(t) = i \int_{-\infty}^\infty \frac{d\lambda}{2\pi} \text{Tr} \left[ G^{(\text{trap})}(\lambda + i0) \right] e^{-i\lambda t}, \quad (8)$$

where the  $i0$  notation means that the integration variable approaches the real axis from above. The Green's function is the solution of Dyson equation, see e.g. Eq.(26) in Ref.[57]. The spectral representation of Green's function without contributions from anti-particle time-backward propagation has the form,

$$G^{(\text{trap})}(\lambda) = \sum_\epsilon \frac{\psi_\epsilon(r) \psi_\epsilon^*(r')}{\epsilon - \lambda}. \quad (9)$$

The trace for non-relativistic trapped systems is defined by,

$$\text{Tr} \left[ G^{(\text{trap})}(\lambda) \right] = \int dr G^{(\text{trap})}(r, r; \lambda). \quad (10)$$

Using the relation between trace of Green's functions and scattering phase shift through a dispersion integral in infinite volume, see e.g. Refs. [1, 57, 58],

$$\text{Tr} \left[ G^{(\infty)}(\epsilon) - G_0^{(\infty)}(\epsilon) \right] = -\frac{1}{\pi} \int_0^\infty d\lambda \frac{\delta(\lambda)}{(\lambda - \epsilon)^2}, \quad (11)$$

we arrive at the final relation in Eq.(1) by,

$$\begin{aligned} C(t) - C_0(t) &= \sum_l \left[ e^{-i\epsilon_l t} - e^{-i\epsilon_l^{(0)} t} \right] \\ &\xrightarrow{\text{trap} \rightarrow \infty} i \int_{-\infty}^\infty \frac{d\lambda}{2\pi} \text{Tr} \left[ G^{(\infty)}(\lambda + i0) - G_0^{(\infty)}(\lambda + i0) \right] e^{-i\lambda t} \\ &= \frac{it}{\pi} \int_0^\infty d\epsilon \delta(\epsilon) e^{-i\epsilon t}. \end{aligned} \quad (12)$$

The  $\epsilon_l$  and  $\epsilon_l^{(0)}$  refer to eigen-energy of interacting and non-interacting particles systems in the trap, respectively.

## III. COUPLED-CHANNEL EXTENSION OF INTEGRATED CORRELATION FUNCTION FORMALISM

The integrated correlation function formalism toward extracting scattering dynamics can in principle be generalized to include coupled-channel inelastic effects in a relatively straightforward manner. We start with Green's

function and its relation to phase shifts that has been worked out in Ref. [58] for coupled channels. To illustrate the main ideas, we will only consider non-relativistic dynamics and two coupled channels in this work. Such a system in an external trap may be described by the Hamiltonian matrix,

$$\hat{H}^{(trap)} = \begin{bmatrix} H_1^{(trap)} + V_1(r) & \gamma(r) \\ \gamma(r) & H_2^{(trap)} + V_2(r) \end{bmatrix}, \quad (13)$$

where  $V_{1,2}(r)$  is the short-range interaction potential in each channel, and  $\gamma(r)$  the interaction potential between the two channels. The  $H_{1,2}^{(trap)}$  is non-interacting trapped Hamiltonian in each channel defined by,

$$H_n^{(trap)} = \sigma_n - \frac{1}{2\mu_n} \frac{d^2}{dr^2} + U_n^{(trap)}(r), \quad n = 1, 2, \quad (14)$$

where  $\sigma_n$  and  $\mu_n$  are threshold energy and reduced mass, and  $U_n^{(trap)}(r)$  the trapping potential, in each channel.

For a coupled-channel system, the integrated two-particle correlation function can still be defined through the trace of Green's function as in Eq.(8), except on the right-hand side of Eq.(8) we have now a matrix of Green's functions.

$$\mathcal{G}^{(trap)}(r, r'; \lambda) = \begin{bmatrix} G_{11}^{(trap)}(r, r'; \lambda) & G_{12}^{(trap)}(r, r'; \lambda) \\ G_{21}^{(trap)}(r, r'; \lambda) & G_{22}^{(trap)}(r, r'; \lambda) \end{bmatrix}, \quad (15)$$

It satisfies the matrix version of Dyson equation,

$$\begin{aligned} \mathcal{G}^{(trap)}(r, r'; \lambda) &= \mathcal{G}_0^{(trap)}(r, r'; \lambda) \\ &+ \int dr'' \mathcal{G}_0^{(trap)}(r, r''; \lambda) V(r'') \mathcal{G}^{(trap)}(r'', r'; \lambda). \end{aligned} \quad (16)$$

The non-interacting Green's function matrix is defined by,

$$\mathcal{G}_0^{(trap)}(r, r'; \lambda) = \begin{bmatrix} G_1^{(trap,0)}(r, r'; \lambda) & 0 \\ 0 & G_2^{(trap,0)}(r, r'; \lambda) \end{bmatrix}, \quad (17)$$

and the potential matrix by,

$$V(r) = \begin{bmatrix} V_1(r) & \gamma(r) \\ \gamma(r) & V_2(r) \end{bmatrix}. \quad (18)$$

The individual channel non-interacting Green's functions in the trap are the solutions of differential equation,

$$\begin{aligned} \left[ \lambda - \sigma_n + \frac{1}{2\mu_n} \frac{d^2}{dr^2} - U_n^{(trap)}(r) \right] G_n^{(trap,0)}(r, r'; \lambda) \\ = \delta(r - r'). \end{aligned} \quad (19)$$

The definition of trace of Green's function matrix must include the trace of the matrix as well. Hence, only diagonal terms of Green's function matrix contribute in the integrated two-particle correlation function,

$$C(t) = i \int_{-\infty}^{\infty} \frac{d\lambda}{2\pi} \left[ \sum_{n=1}^2 \int dr G_{nn}^{(trap)}(r, r; \lambda + i0) \right] e^{-i\lambda t}. \quad (20)$$

In the following two subsections, we will connect the difference of integrated correlation functions between interacting and non-interacting particles systems and phase shifts in the coupled channels as the infinite volume limit is approached, just as in single-channel cases.

### A. Coupled-channel scattering solutions in infinite volume

As detailed in Ref. [58], in the case of short-range interaction, the infinite volume scattering solutions for coupled-channel dynamics can be worked out straightforwardly. Here, we briefly outline the main results. The scattering coupled-channel wavefunctions can be determined by Lippmann-Schwinger equations,

$$\begin{aligned} \begin{bmatrix} \psi_1^{(\infty)}(r; E) \\ \psi_2^{(\infty)}(r; E) \end{bmatrix} &= \begin{bmatrix} \psi_1^{(\infty,0)}(r; E) \\ \psi_2^{(\infty,0)}(r; E) \end{bmatrix} \\ &+ \int dr' \begin{bmatrix} G_1^{(\infty,0)}(r - r'; E) & 0 \\ 0 & G_2^{(\infty,0)}(r - r'; E) \end{bmatrix} \\ &\times \begin{bmatrix} V_1(r') & \gamma(r') \\ \gamma(r') & V_2(r') \end{bmatrix} \begin{bmatrix} \psi_1^{(\infty)}(r'; E) \\ \psi_2^{(\infty)}(r'; E) \end{bmatrix}, \end{aligned} \quad (21)$$

where the infinite volume free-particle Green's function in individual channel is defined by

$$\begin{aligned} G_n^{(\infty,0)}(x; E + i0) \\ = \int \frac{dp}{2\pi} \frac{e^{ipx}}{E - \sigma_n - \frac{p^2}{2\mu_n} + i0} = -\frac{i\mu_n}{k_n} e^{ik_n|x|}. \end{aligned} \quad (22)$$

The total energy is related to the threshold energy and relative momentum in each channel by the dispersion relation,

$$E = \sigma_n + \frac{k_n^2}{2\mu_n}, \quad n = 1, 2. \quad (23)$$

The scattering amplitudes are defined through the asymptotic behavior of wavefunction solutions by considering two sets of independent boundary conditions of incoming waves:

$$\begin{aligned} (1) \quad \begin{bmatrix} \psi_1^{(\infty,0)}(r; E) \\ \psi_2^{(\infty,0)}(r; E) \end{bmatrix} &= \begin{bmatrix} e^{ik_1 r} \\ 0 \end{bmatrix}, \\ (2) \quad \begin{bmatrix} \psi_1^{(\infty,0)}(r; E) \\ \psi_2^{(\infty,0)}(r; E) \end{bmatrix} &= \begin{bmatrix} 0 \\ e^{ik_2 r} \end{bmatrix}. \end{aligned} \quad (24)$$

Under these conditions, the asymptotic solutions of wavefunctions can be written as,

$$\begin{aligned} (1) \quad \begin{bmatrix} \psi_1^{(\infty)}(r; E) \\ \psi_2^{(\infty)}(r; E) \end{bmatrix} \Big|_{r \rightarrow \infty} &= \begin{bmatrix} e^{ik_1 r} + i \frac{\mu_1}{k_1} T_{11} e^{ik_1 |r|} \\ i \frac{\mu_2}{k_2} T_{21} e^{ik_2 |r|} \end{bmatrix}, \\ (2) \quad \begin{bmatrix} \psi_1^{(\infty)}(r; E) \\ \psi_2^{(\infty)}(r; E) \end{bmatrix} \Big|_{r \rightarrow \infty} &= \begin{bmatrix} i \frac{\mu_1}{k_1} T_{12} e^{ik_1 |r|} \\ e^{ik_2 r} + i \frac{\mu_2}{k_2} T_{22} e^{ik_2 |r|} \end{bmatrix}. \end{aligned} \quad (25)$$

The coupled-channel scattering amplitudes (T-matrix elements) can be parameterized by two phase shifts,  $\delta_{1,2}$ , and one inelasticity,  $\eta \in [0, 1]$ , see e.g. [10, 11, 59–61],

$$\begin{aligned} T_{11} &= \frac{k_1}{\mu_1} \frac{\eta e^{2i\delta_1} - 1}{2i}, & T_{22} &= \frac{k_2}{\mu_2} \frac{\eta e^{2i\delta_2} - 1}{2i}, \\ T_{12} = T_{21} &= \sqrt{\frac{k_1 k_2}{\mu_1 \mu_2}} \frac{\sqrt{1 - \eta^2} e^{i(\delta_1 + \delta_2)}}{2}. \end{aligned} \quad (26)$$

We remark that short-range interactions have been assumed, so only even-parity solutions are contributing. The  $S$ -matrix is defined by, see e.g. Ref. [58],

$$\begin{aligned} S(E) &= \begin{bmatrix} 1 + 2i \frac{\mu_1}{k_1} T_{11} & 2i \sqrt{\frac{\mu_1 \mu_2}{k_1 k_2}} T_{12} \\ 2i \sqrt{\frac{\mu_1 \mu_2}{k_1 k_2}} T_{21} & 1 + 2i \frac{\mu_2}{k_2} T_{22} \end{bmatrix} \\ &= \begin{bmatrix} \eta e^{2i\delta_1} & i \sqrt{1 - \eta^2} e^{i(\delta_1 + \delta_2)} \\ i \sqrt{1 - \eta^2} e^{i(\delta_1 + \delta_2)} & \eta e^{2i\delta_2} \end{bmatrix}, \end{aligned} \quad (27)$$

and it satisfies the unitarity relation  $S^\dagger(E)S(E) = 1$ .

The infinite volume Green's functions for coupled-channel system satisfy the similar matrix version of Dyson equation as in trapped systems. As shown in Ref. [58], the trace of the difference of integrated Green's function between interacting and non-interacting systems is related to two scattering phase shifts by a dispersion relation, also known as Krein's theorem [62] in spectral theory,

$$\begin{aligned} \text{Tr} \left[ \mathcal{G}^{(\infty)}(E) - \mathcal{G}_0^{(\infty)}(E) \right] &= \sum_{n=1}^2 \int_{-\infty}^{\infty} dr \left[ G_{nn}^{(\infty)}(r, r; E) - G_n^{(\infty,0)}(0; E) \right] \\ &= -\frac{1}{\pi} \int_{\sigma_1}^{\infty} d\lambda \frac{\delta_1(\lambda)}{(\lambda - E)^2} - \frac{1}{\pi} \int_{\sigma_2}^{\infty} d\lambda \frac{\delta_2(\lambda)}{(\lambda - E)^2}, \end{aligned} \quad (28)$$

whose absorptive part,

$$\begin{aligned} \text{Im} \left[ \text{Tr} \left[ \mathcal{G}^{(\infty)}(E) - \mathcal{G}_0^{(\infty)}(E) \right] \right] &= \sum_{n=1}^2 \int_{-\infty}^{\infty} dr \text{Im} \left[ G_{nn}^{(\infty)}(r, r; E) - G_n^{(\infty,0)}(0; E) \right] \\ &= -\frac{d}{dE} [\delta_1(E) + \delta_2(E)], \end{aligned} \quad (29)$$

gives the coupled-channel version of Friedel formula [63–65] in condensed matter theory, also see discussions in e.g. Ref. [57]. Combining the definition of  $C(t)$  in Eq.(20) and Eq.(28) yields the final relation in Minkowski space,

$$C(t) - C_0(t) \xrightarrow{\text{trap} \rightarrow \infty} \frac{it}{\pi} \left[ \int_{\sigma_1}^{\infty} \delta_1(\epsilon) + \int_{\sigma_2}^{\infty} \delta_2(\epsilon) \right] e^{-i\epsilon t} d\epsilon, \quad (30)$$

The corresponding relation in Euclidean space is given by,

$$C(\tau) - C_0(\tau) \xrightarrow{\text{trap} \rightarrow \infty} \frac{\tau}{\pi} \left[ \int_{\sigma_1}^{\infty} \delta_1(\epsilon) + \int_{\sigma_2}^{\infty} \delta_2(\epsilon) \right] e^{-\epsilon \tau} d\epsilon. \quad (31)$$

Eq.(31) is the main result of this work. In the following, we will examine its properties from multiple angles.

## B. Energy spectrum representation of integrated correlation function and quantization condition

For trapped systems, similar to the single-channel spectral representation, see e.g. Ref. [1], the spectral representation of full Green's function matrix is given by,

$$\mathcal{G}^{(\text{trap})}(r, r'; \lambda) = \sum_l \frac{\psi^{(\text{trap})}(r; \epsilon_l) \psi^{(\text{trap})\dagger}(r'; \epsilon_l)}{\lambda - \epsilon_l}, \quad (32)$$

where

$$\psi^{(\text{trap})}(r; \epsilon) = \begin{bmatrix} \psi_1^{(\text{trap})}(r; \epsilon) \\ \psi_2^{(\text{trap})}(r; \epsilon) \end{bmatrix}, \quad (33)$$

stands for a column matrix of coupled-channel wavefunctions, and is the eigen-solution of coupled-channel Schrödinger equation,

$$\hat{H}^{(\text{trap})} \psi^{(\text{trap})}(r; \epsilon_l) = \epsilon_l \psi^{(\text{trap})}(r; \epsilon_l). \quad (34)$$

The normalization condition for the wavefunctions of coupled-channel systems is given by

$$\int dr \psi^{(\text{trap})\dagger}(r; \epsilon_l) \psi^{(\text{trap})}(r; \epsilon_{l'}) = \delta_{l,l'}, \quad (35)$$

which leads to the trace,

$$\text{Tr} \left[ \mathcal{G}^{(\text{trap})}(\lambda) \right] = \sum_{n=1}^2 \int dr G_{nn}^{(\text{trap})}(r, r; \lambda) = \sum_l \frac{1}{\lambda - \epsilon_l}. \quad (36)$$

Using the definition of the integrated correlation function for coupled-channel system in Eq.(20), we thus find the energy spectrum representation of integrated correlation function for coupled-channel system:

$$C(t) = \sum_l e^{-i\epsilon_l t}. \quad (37)$$

It resembles the result in single-channel systems in Eq.(7), but now  $\epsilon$  stands for the discrete eigen-energies in coupled-channel systems. Therefore, similar to relation in Eq.(12) in single-channel cases, we find a useful relation,

$$\begin{aligned} &\sum_l \left[ e^{-i\epsilon_l t} - e^{-i\epsilon_l^{(0)} t} \right] \\ &\xrightarrow{\text{trap} \rightarrow \infty} \frac{it}{\pi} \left[ \int_{\sigma_1}^{\infty} \delta_1(\epsilon) + \int_{\sigma_2}^{\infty} \delta_2(\epsilon) \right] e^{-i\epsilon t} d\epsilon, \end{aligned} \quad (38)$$

for coupled-channel systems in terms of energy spectra. The eigen-energy of coupled-channel systems in a trap can be solved by diagonalizing the Hamiltonian in the

basis of non-interacting trapped systems. Expanding coupled-channel wavefunctions,

$$\psi^{(trap)}(r; \epsilon) = \sum_l \begin{bmatrix} c_l^{(1)} \phi_l^{(1)}(r) \\ c_l^{(2)} \phi_l^{(2)}(r) \end{bmatrix}, \quad (39)$$

in terms of the eigen-solution of Schrödinger equation for non-interacting trapped systems,

$$H_n^{(trap)} \phi_l^{(n)}(r) = \epsilon_l^{(n,0)} \phi_l^{(n)}(r), \quad n = 1, 2, \quad (40)$$

the Schrödinger equation in Eq.(34) is converted to a matrix equation,

$$\sum_{l'} H_{l,l'}^{(trap)} \begin{bmatrix} c_{l'}^{(1)} \\ c_{l'}^{(2)} \end{bmatrix}_m = \epsilon_m \begin{bmatrix} c_l^{(1)} \\ c_l^{(2)} \end{bmatrix}_m, \quad (41)$$

where  $\epsilon_m$  is the  $m$ -th eigen-energy of this equation, different from  $\epsilon_l^{(n,0)}$ . The matrix element of Hamiltonian in the basis of non-interacting trapped systems is thus given by (omitting the label trap),

$$H_{l,l'} = \begin{bmatrix} \delta_{l,l'} \epsilon_l^{(1,0)} + V_{l,l'}^{(1)} & \gamma_{l,l'} \\ \gamma_{l',l}^* & \delta_{l,l'} \epsilon_l^{(2,0)} + V_{l,l'}^{(2)} \end{bmatrix}, \quad (42)$$

where the matrix elements  $V_{l,l'}^{(1,2)}$  and  $\gamma_{l,l'}$  are defined by

$$\begin{aligned} V_{l,l'}^{(n)} &= \int dr \phi_l^{(n)*}(r) V_n(r) \phi_{l'}^{(n)}(r), \quad n = 1, 2, \\ \gamma_{l,l'} &= \int dr \phi_l^{(2)*}(r) \gamma(r) \phi_{l'}^{(1)}(r). \end{aligned} \quad (43)$$

On the other hand, as discussed in Ref. [1, 2], also see relevant discussions in e.g. Ref. [25–28, 61, 66–68], when the size of the trap is much larger than the range of interaction, the short-range interaction potential can be well approximated by contact interactions,

$$V(r) = \begin{bmatrix} V_1 \delta(r) & \gamma \delta(r) \\ \gamma \delta(r) & V_2 \delta(r) \end{bmatrix}. \quad (44)$$

The quantization condition that determines the discrete eigen-energy for trapped systems can be derived through homogeneous Lippmann-Schwinger equations [61, 66, 67], which reads in our notation,

$$\det \left[ \begin{bmatrix} V_1 & \gamma \\ \gamma & V_2 \end{bmatrix}^{-1} - \begin{bmatrix} G_1^{(trap,0)}(0,0;\epsilon) & 0 \\ 0 & G_2^{(trap,0)}(0,0;\epsilon) \end{bmatrix} \right] = 0. \quad (45)$$

The relation between interaction potentials and infinite volume scattering amplitudes matrix can be readily established with contact interaction approximation [61, 66, 67],

$$-\begin{bmatrix} V_1 & \gamma \\ \gamma & V_2 \end{bmatrix}^{-1} = T^{-1} + \begin{bmatrix} \frac{i\mu_1}{k_1} & 0 \\ 0 & \frac{i\mu_2}{k_2} \end{bmatrix}. \quad (46)$$

Eliminating interaction potential matrix in Eq.(45) and Eq.(46), and also using phase shift and inelasticity parametrization of  $T$ -matrix in Eq.(26), the quantization condition for coupled-channel system can be written in a compact form,

$$\begin{aligned} &\eta(1 + g_1 g_2) \cos(\delta_1 - \delta_2) + (1 - g_1 g_2) \cos(\delta_1 + \delta_2) \\ &- \eta(g_1 - g_2) \sin(\delta_1 - \delta_2) - (g_1 + g_2) \sin(\delta_1 + \delta_2) = 0, \end{aligned} \quad (47)$$

where the  $g_{1,2}$  functions are defined by

$$g_n = -\frac{k_n}{\mu_n} G_0^{(trap,0)}(0, 0; \epsilon), \quad n = 1, 2. \quad (48)$$

The quantization condition in Eq.(47) has the same structure as in Eq.(25) in Ref. [10] for finite volume coupled-channel systems and Eq.(51) in Ref. [61] for coupled-channel systems in a harmonic oscillator trap, providing an independent confirmation of our formalism. The  $g_{1,2}$  functions play the role of Lüscher zeta function in the finite volume system [3]. Explicitly in 1D periodic box of size  $L$ , the functions are [18–21],

$$g_n = -\cot \left( \frac{L}{2} \sqrt{2\mu_n(\epsilon - \sigma_n)} \right). \quad (49)$$

For the harmonic trap with angular frequency  $\omega$ , explicit expressions for  $g_{1,2}$  functions are given by

$$g_n = \sqrt{\frac{\epsilon - \sigma_n}{2\omega}} \frac{\Gamma(\frac{1}{4} - \frac{\epsilon - \sigma_n}{2\omega})}{\Gamma(\frac{3}{4} - \frac{\epsilon - \sigma_n}{2\omega})}, \quad (50)$$

which is the periodic function known as BREW formula in single channel [61, 66, 69]. When the coupling between the two channels is turned off ( $\gamma = 0$ ), the coupled-channel quantization condition in Eq.(47) is reduced to the well-known single-channel Lüscher formula:  $\cot \delta_n = g_n$ , see e.g. Refs. [3, 61, 66, 69].

### C. Example of an exactly solvable model

Having obtained the relation in Eq.(31), we want to check its convergence by an exactly solvable model. With the contact interaction potentials in Eq.(44), the analytic solutions of infinite volume scattering amplitudes are available via Eq.(46):

$$T = -\begin{bmatrix} V_1 & \gamma \\ \gamma & V_2 \end{bmatrix} \begin{bmatrix} 1 + \frac{i\mu_1}{k_1} V_1 & \frac{i\mu_1}{k_1} \gamma \\ \frac{i\mu_2}{k_2} \gamma & 1 + \frac{i\mu_2}{k_2} V_2 \end{bmatrix}^{-1}. \quad (51)$$

The T-matrix elements are given by,

$$\begin{aligned} T_{11}(\epsilon) &= \frac{k_1}{\mu_1} \frac{i(\gamma^2 - V_1 V_2) - V_1 \frac{k_2}{\mu_2}}{(\frac{k_1}{\mu_1} + iV_1)(\frac{k_2}{\mu_2} + iV_2) + \gamma^2}, \\ T_{12}(\epsilon) &= T_{21}(\epsilon) = \frac{-\gamma \frac{k_1}{\mu_1} \frac{k_2}{\mu_2}}{(\frac{k_1}{\mu_1} + iV_1)(\frac{k_2}{\mu_2} + iV_2) + \gamma^2}, \\ T_{22}(\epsilon) &= \frac{k_2}{\mu_2} \frac{i(\gamma^2 - V_1 V_2) - V_2 \frac{k_1}{\mu_1}}{(\frac{k_1}{\mu_1} + iV_1)(\frac{k_2}{\mu_2} + iV_2) + \gamma^2}, \end{aligned} \quad (52)$$

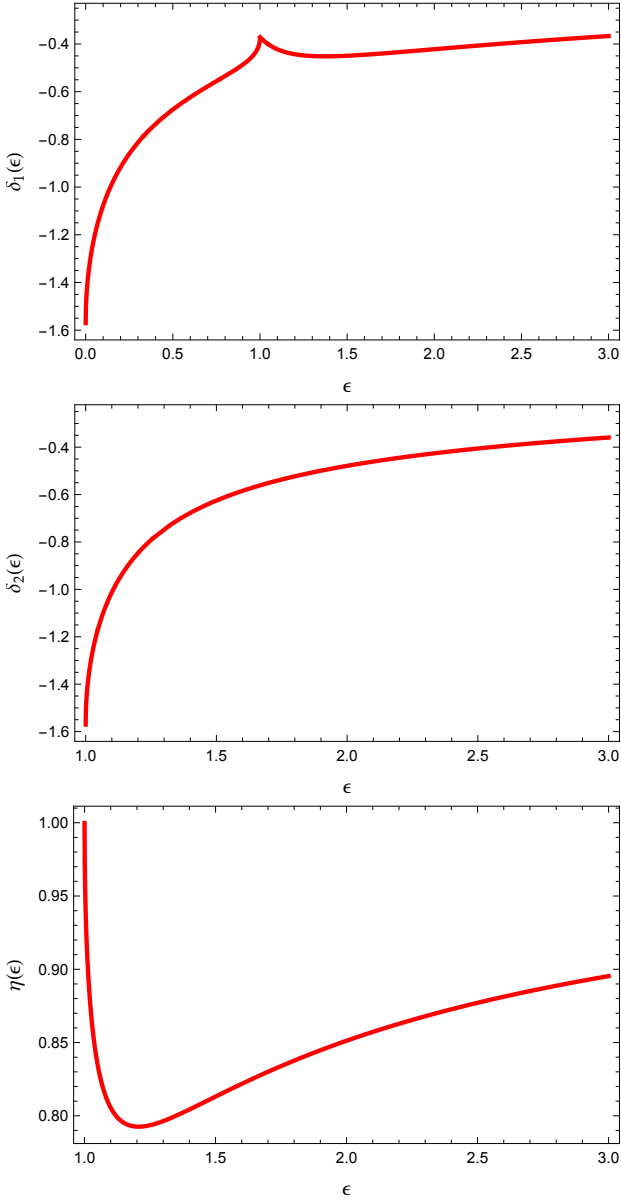


FIG. 1: Model parameters for phase shifts ( $\delta_1$  and  $\delta_2$ ) and inelasticity ( $\eta$ ) as defined in Eq.(55). The kink in  $\delta_1$  is a threshold effect corresponding to the dip in  $\eta$ . Other parameters are taken as:  $V_1 = 1.0$ ,  $V_2 = 0.8$ ,  $\gamma = 0.6$ ,  $\sigma_1 = 0$ ,  $\sigma_2 = 1$  and  $\mu_1 = \mu_2 = 1$ .

where  $k_n = \sqrt{2\mu_n(\epsilon - \sigma_n)}$ . The  $S$ -matrix elements are,

$$\begin{aligned}
 S_{11}(\epsilon) &= \frac{\left(\frac{k_1}{\mu_1} - iV_1\right)\left(\frac{k_2}{\mu_2} + iV_2\right) - \gamma^2}{\left(\frac{k_1}{\mu_1} + iV_1\right)\left(\frac{k_2}{\mu_2} + iV_2\right) + \gamma^2}, \\
 S_{12}(\epsilon) = S_{21}(\epsilon) &= \frac{-2i\gamma\sqrt{\frac{k_1}{\mu_1}\frac{k_2}{\mu_2}}}{\left(\frac{k_1}{\mu_1} + iV_1\right)\left(\frac{k_2}{\mu_2} + iV_2\right) + \gamma^2}, \\
 S_{22}(\epsilon) &= \frac{\left(\frac{k_1}{\mu_1} + iV_1\right)\left(\frac{k_2}{\mu_2} - iV_2\right) - \gamma^2}{\left(\frac{k_1}{\mu_1} + iV_1\right)\left(\frac{k_2}{\mu_2} + iV_2\right) + \gamma^2}.
 \end{aligned} \tag{53}$$

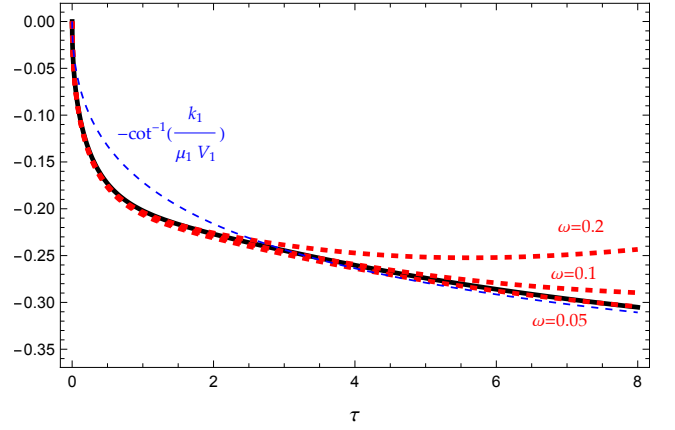


FIG. 2: Convergence check of Eq.(31) in an exactly solvable model. The dashed red lines are the difference  $C(t) - C_0(t)$  on the left-hand-side in harmonic oscillator trap with  $\omega = 0.05, 0.1, 0.2$ . The solid black curve is the full result in infinite volume limit on the right-hand-side. The parameters are taken as:  $V_1 = 0.6$ ,  $V_2 = 0.3$ ,  $\gamma = 0.2$ ,  $\sigma_1 = 0$ ,  $\sigma_2 = 1$ , and  $\mu_1 = \mu_2 = 1$ . The dashed blue curve is the phase shift of channel-1 when the inelastic effect is turned off ( $V_2 = 0, \gamma = 0$ ).

The scattering amplitudes satisfy the unitarity relation,

$$\text{Im} [T_{nn'}(\epsilon)] = \sum_{l=1}^2 \theta(\epsilon - \sigma_l) \frac{\mu_l}{k_l} T_{nl}^*(\epsilon) T_{ln'}(\epsilon). \tag{54}$$

The inelasticity and two-channel phase shifts can thus be computed by

$$\begin{aligned}
 \eta(\epsilon) &= \begin{cases} \sqrt{1 - 4\frac{\mu_1}{k_1}\frac{\mu_2}{k_2}|T_{12}(\epsilon)|^2}, & \text{if } \epsilon > \sigma_2, \\ 1, & \text{otherwise,} \end{cases} \\
 \delta_n(\epsilon) &= \begin{cases} \frac{1}{2i} \ln \left[ \frac{1 + 2i\frac{\mu_n}{k_n} T_{nn}(\epsilon)}{\eta(\epsilon)} \right], & \text{if } \epsilon > \sigma_n, \\ 0, & \text{otherwise.} \end{cases}
 \end{aligned} \tag{55}$$

For the contact interaction in 1D, the phase shifts approach  $-\frac{\pi}{2}$  at thresholds:  $\delta_n(\sigma_n) = -\frac{\pi}{2}$ . An example for the real parts of the phase shifts and inelasticity as a function of energy is plotted in Fig. 1.

If harmonic oscillator trap is used, the basis functions are explicitly given by,

$$\phi_l^{(n)}(r) = \frac{1}{\sqrt{2^l l!}} \left( \frac{\mu_n \omega}{\pi} \right)^{\frac{1}{4}} e^{-\frac{\mu_n \omega}{2} r^2} H_l(\sqrt{\mu_n \omega} r), \quad n = 1, 2. \tag{56}$$

with associated energies  $\epsilon_l^{(\omega)} = \omega(l + \frac{1}{2})$ . Hence, the Hamiltonian matrix for coupled-channel system with contact interactions in harmonic oscillator trap is given by,

$$H_{l,l'} = \begin{bmatrix} \delta_{l,l'}(\sigma_1 + \epsilon_l^{(\omega)}) + V_{l,l'}^{(1)} & \gamma_{l,l'} \\ \gamma_{l',l} & \delta_{l,l'}(\sigma_2 + \epsilon_l^{(\omega)}) + V_{l,l'}^{(2)} \end{bmatrix}, \tag{57}$$



where matrix elements of potential terms can be evaluated by Eq.(43). The interacting trapped integrated correlation function in Euclidean time, see Eq.(37),

$$C(\tau) = \sum_l e^{-E_l \tau}, \quad (58)$$

can be computed by using energy spectrum  $\{E_l\}$  by diagonalizing the Hamiltonian in Eq.(57). The non-interacting version is given by,

$$C_0(\tau) = (e^{-\sigma_1 \tau} + e^{-\sigma_2 \tau}) \frac{1}{2} \text{csch}\left(\frac{\omega \tau}{2}\right), \quad (59)$$

where we have used the identity:

$$\sum_l e^{-\omega(l+\frac{1}{2})\tau} = \frac{1}{2} \text{csch}\left(\frac{\omega \tau}{2}\right).$$

Eq.(58) and Eq.(59) will be further elucidated in the path integral representation below.

A numerical demonstration of the relation in Eq.(31) is shown in Fig. 2 using the coupled-channel parametrization in Fig. 1. The  $C(\tau)$  is computed by feeding  $\{E_l\}$  into Eq.(58) as mentioned above. The  $C_0(\tau)$  is computed by Eq.(59). The results with various size of harmonic oscillator traps,  $\omega \in [0.005, 0.1, 0.2]$ , are compared with its infinite volume limit on the right-hand-side using the phase shifts in Eq.(55). We see that as  $\omega \rightarrow 0$  (which corresponds to trap  $\rightarrow \infty$ ), the relation is satisfied. Even with relative large trap size of  $\omega \sim 0.2$ , the difference of integrated correlation functions shows a rapid convergence to its infinite volume limit near short times. To highlight the inelastic effect, the phase shift of channel-1 from turning off inelastic dynamics ( $V_2 = \gamma = 0$ ),

$$\delta_1 \xrightarrow{(V_2, \gamma) \rightarrow 0} -\cot^{-1}\left(\frac{k_1}{\mu_1 V_1}\right), \quad (60)$$

is also plotted in Fig. 2. Sizable inelastic effect is observed at short times.

#### IV. MONTE CARLO SIMULATION OF A QUASI-ONE-DIMENSIONAL COUPLED-CHANNEL MODEL

In this section, we propose a quasi-one-dimensional quantum mechanical model to further validate the coupled-channel dynamics when the system is not exactly solvable. Here ‘quasi’ means that the coupled-channel 1D dynamics is embedded in a two-dimensional (2D) waveguide model [58]. In the following, we will show that when the particles are confined in a 2D trap, the number of bound states in the transverse direction can be manipulated in the path integral representation and its degrees of freedom can be integrated out, reducing the 2D system to a quasi-1D coupled-channel quantum mechanical system, which can be used to conduct nontrivial tests on the proposed coupled-channel formalism.

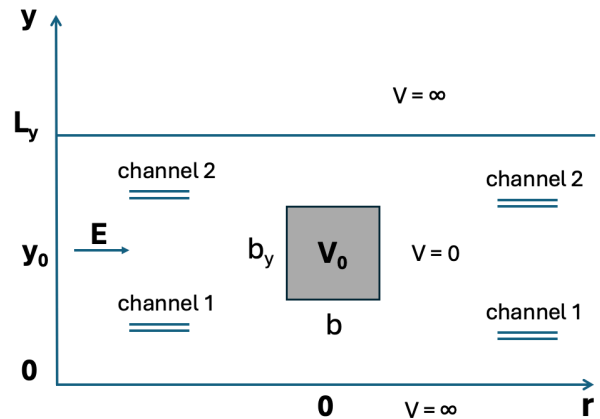


FIG. 3: Illustration of quasi-one-dimensional coupled-channel system that is embedded in a 2D geometry. The grey square in the middle represents the 2D square-well interaction potential placed at  $(0, y_0)$  that yields the coupled-channel interaction potentials in quasi-1D. Each channel is a two-particle system with total energy  $E$  and individual ones as related in Eq.(23). The system is confined in  $y$ -direction by a hard-wall trap of width  $L_y$  and a harmonic oscillator trap in  $r$ -direction.

##### A. Quasi-1D quantum mechanical model

Following Ref. [58], the quasi-1D system can be described by a 2D Hamiltonian,

$$\hat{H} = \hat{H}_r^{(\omega)} + \hat{H}_y^{(trap)} + V(r, y), \quad (61)$$

where

$$\hat{H}_r^{(\omega)} = -\frac{1}{2m} \frac{\partial^2}{\partial r^2} + \frac{1}{2} m \omega^2 r^2, \quad (62)$$

describes a harmonic oscillator trap in  $r$ -direction, and,

$$\hat{H}_y^{(trap)} = -\frac{1}{2m} \frac{\partial^2}{\partial y^2} + U_y^{(trap)}(y), \quad (63)$$

a trap in  $y$ -direction whose form can be chosen. The  $V(r, y)$  is used to simulate the short-range interaction between the two particles. In this work, we use a simple 2D square-well potential,

$$V(r, y) = \begin{cases} \frac{V_0}{bb_y}, & \text{if } r \in [-\frac{b}{2}, \frac{b}{2}] \& y \in [y_0 - \frac{b_y}{2}, y_0 + \frac{b_y}{2}], \\ 0, & \text{otherwise,} \end{cases} \quad (64)$$

where  $b$  and  $b_y$  are the width of square well along  $r$ - and  $y$ -direction respectively. The center of the square well is placed at  $(0, y_0)$ . The schematic diagram with a hard-wall trap in  $y$ -direction is shown in Fig. 3. At the limit of shrinking width of square well from both directions, the above potential is reduced to a 2D  $\delta$ -potential,

$$V(r, y) \xrightarrow{(b, b_y) \rightarrow 0} V_0 \delta(r) \delta(y - y_0), \quad (65)$$

whose eigenstates have only even parity [1].

We assume that only two lowest bound states in  $y$ -direction are contributing, although this number can be manipulated in Monte Carlo simulation to be discussed next. The two bound states are the solutions of,

$$\hat{H}_y^{(trap)}\chi_n(y) = \sigma_n\chi_n(y), \quad n = 1, 2. \quad (66)$$

The total 2D wavefunction can be written in the form of,

$$\Psi_E(r, y) = \sum_{n=1}^2 \psi_E^{(n)}(r)\chi_n(y), \quad (67)$$

where  $n$  labels the  $n$ -th channel in  $r$ -direction. After integrating out dynamics along  $y$ -direction, we find,

$$\sum_{n'=1}^2 \left[ \delta_{n,n'}(\sigma_n + \hat{H}_r^{(\omega)}) + V_{n,n'}(r) \right] \psi_E^{(n')}(r) = E\psi_E^{(n)}(r), \quad (68)$$

where

$$V_{n,n'}(r) = \int_{y_0 - \frac{by}{2}}^{y_0 + \frac{by}{2}} dy \chi_n^*(y)V(r, y)\chi_{n'}(y). \quad (69)$$

The quasi-1D coupled-channel dynamics can indeed be reduced from 2D systems. Hence the coupled-channel dynamics may be simulated and tested in 2D quantum mechanics by Monte Carlo methods.

### B. Path integral representation of quasi-1D quantum mechanical model

In Euclidean space-time, the path integral representation of transition amplitude for a single particle propagating from  $(r, y, 0)$  to  $(r', y', \tau)$  is defined by,

$$\begin{aligned} \langle r', y' | e^{-\hat{H}\tau} | r, y \rangle &= \int \prod_{i=1}^{N_\tau-1} dr_i dy_i e^{-S_E^{(\omega)}(\{r_i\})} \\ &\times \rho(y, y_1; a_\tau) \cdots \rho(y_{N_\tau-1}, y'; a_\tau) e^{-S_E^{(V)}(\{r_i, y_i\})}, \end{aligned} \quad (70)$$

where the time interval  $[0, \tau]$  is discretized by a one-dimensional lattice of  $N_\tau$  small steps of spacing  $a_\tau = \frac{\tau}{N_\tau}$ . The Euclidean space-time harmonic oscillator trapped action in  $r$ -direction is given by,

$$S_E^{(\omega)}(\{r_i\}) = a_\tau \sum_{i=1}^{N_\tau} \left[ \frac{m}{2} \left( \frac{r_{i+1} - r_i}{a_\tau} \right)^2 + \frac{1}{2} m \omega^2 r_i^2 \right], \quad (71)$$

and the interaction action by,

$$S_E^{(V)}(\{r_i, y_i\}) = a_\tau \sum_{i=1}^{N_\tau} V(r_i, y_i). \quad (72)$$

The density matrix in  $y$ -direction is defined by,

$$\rho(y_1, y_2; a_\tau) = \sum_{n=1}^2 e^{-\sigma_n a_\tau} \chi_n(y_1) \chi_n^*(y_2), \quad (73)$$

which obeys the relation on the lattice,

$$\int \prod_{i=1}^{N_\tau-1} dy_i \rho(y, y_1; a_\tau) \cdots \rho(y_{N_\tau-1}, y'; a_\tau) = \rho(y, y'; \tau). \quad (74)$$

The spectral representation of transition amplitude is given by,

$$\langle r', y' | e^{-\hat{H}\tau} | r, y \rangle = \sum_l e^{-E_l \tau} \Psi_l(r, y) \Psi_l^*(r', y'), \quad (75)$$

where  $E_l$  and  $\Psi_l(r, y)$  are eigen-energy and eigen-wavefunction of trapped system:  $\hat{H}\Psi_l(r, y) = E_l\Psi_l(r, y)$ . In this representation, the integrated particle propagator takes the form,

$$C(\tau) = \int dr dy \langle r, y | e^{-\hat{H}\tau} | r, y \rangle = Tr[e^{-\hat{H}\tau}] = \sum_l e^{-E_l \tau}. \quad (76)$$

The ratio of integrated particle propagators can be expressed as,

$$\frac{C(\tau)}{C_0(\tau)} = \int \prod_{i=1}^{N_\tau} dr_i dy_i p(\{r_i, y_i\}) e^{-S_E^{(V)}(\{r_i, y_i\})}, \quad (77)$$

where  $r_{N_\tau} = r = r'$  and  $y_{N_\tau} = y = y'$ , and the probability density distribution is defined by,

$$\begin{aligned} p(\{r_i, y_i\}) &= \frac{e^{-S_E^{(\omega)}(\{r_i\})} \rho(y_{N_\tau}, y_1; a_\tau) \cdots \rho(y_{N_\tau-1}, y_{N_\tau}; a_\tau)}{C_0(\tau)}. \end{aligned} \quad (78)$$

In this way, the interaction action factor  $e^{-S_E^{(V)}}$  and the harmonic trap action factor  $e^{-S_E^{(\omega)}}$  are separated. The  $C_0(\tau)$  represents the non-interacting integrated particle propagator,

$$C_0(\tau) = C_0^{(\omega)}(\tau) C_0^{(y)}(\tau) = Tr[e^{-\hat{H}_0 \tau}], \quad (79)$$

where

$$C_0^{(\omega)}(\tau) = \int \prod_{i=1}^{N_\tau} dr_i e^{-S_E^{(\omega)}(\{r_i\})} = \sum_{l=0}^{\infty} e^{-\omega(l+\frac{1}{2})\tau}, \quad (80)$$

and

$$\begin{aligned} C_0^{(y)}(\tau) &= \int \prod_{i=1}^{N_\tau} dy_i \rho(y_{N_\tau}, y_1; a_\tau) \cdots \rho(y_{N_\tau-1}, y_{N_\tau}; a_\tau) \\ &= e^{-\sigma_1 \tau} + e^{-\sigma_2 \tau}. \end{aligned} \quad (81)$$



As a consequence, the probability density distribution is positive-definite and normalized,

$$\int \prod_{i=1}^{N_\tau} dr_i dy_i p(\{r_i, y_i\}) = 1, \quad (82)$$

This property suggests that Eq.(77) can in principle be evaluated via Monte Carlo methods.

Furthermore, Eq.(77) can be simplified by integrating out dynamical degrees of freedom in  $y$ -direction by defining effective potentials in  $r$ -direction,

$$\int dy_1 |\chi_n(y_1)|^2 e^{-a_\tau V(r_1, y_1)} = e^{-a_\tau V_n(r_1)}, \quad n = 1, 2, \quad (83)$$

and,

$$\int dy_1 \chi_1(y_1) e^{-a_\tau V(r_1, y_1)} \chi_2^*(y_1) = -a_\tau \gamma(r_1). \quad (84)$$

Since wavefunctions  $\chi_n(y)$  are real functions,  $V_{1,2}(r_1)$  and  $\gamma(r_1)$  are real effective potentials. Due to orthogonality of  $\chi_l(y)$  functions, the effective potentials still have square-well form,

$$V_n(r_1) = \begin{cases} -\frac{\ln \left[ 1 + \kappa_n \left( e^{-\frac{a_\tau V_0}{bb_y}} - 1 \right) \right]}{a_\tau}, & \text{if } r_1 \in \left[ -\frac{b}{2}, \frac{b}{2} \right], \\ 0, & \text{otherwise,} \end{cases}$$

$$\gamma(r_1) = \begin{cases} -\frac{\kappa_\gamma \left( e^{-\frac{a_\tau V_0}{bb_y}} - 1 \right)}{a_\tau}, & \text{if } r_1 \in \left[ -\frac{b}{2}, \frac{b}{2} \right], \\ 0, & \text{otherwise,} \end{cases} \quad (85)$$

where the coefficients are defined by,

$$\kappa_n = \int_{y_0 - \frac{b_y}{2}}^{y_0 + \frac{b_y}{2}} dy_1 |\chi_n(y_1)|^2, \quad n = 1, 2,$$

$$\kappa_\gamma = \int_{y_0 - \frac{b_y}{2}}^{y_0 + \frac{b_y}{2}} dy_1 \chi_1(y_1) \chi_2^*(y_1). \quad (86)$$

The introduction of effective potentials leads to  $y$ -integration that can be expressed in matrix form,

$$\int dy_1 \rho(y_0, y_1; a_\tau) e^{-aV(r_1, y_1)} \rho(y_1, y_2; a_\tau) = [\chi_1(y_2) \quad \chi_2(y_2)] M(r_1) \begin{bmatrix} \chi_1(y_0) e^{-\sigma_1 a_\tau} \\ \chi_2(y_0) e^{-\sigma_2 a_\tau} \end{bmatrix}, \quad (87)$$

where  $M(r_1)$  is defined by,

$$M(r_1) = \begin{bmatrix} e^{-aV_1(r_1)} e^{-\sigma_1 a_\tau} & -a\gamma(r_1) e^{-\sigma_1 a_\tau} \\ -a\gamma(r_1) e^{-\sigma_2 a_\tau} & e^{-aV_2(r_1)} e^{-\sigma_2 a_\tau} \end{bmatrix}. \quad (88)$$

Carrying out all  $y$ -direction integrations step by step, we find,

$$\int \prod_{i=1}^{N_\tau} dy_i \rho(y_{N_\tau}, y_1; a_\tau) \cdots \rho(y_{N_\tau}, y_{N_\tau}; a_\tau) e^{-S_E^{(V)}(\{r_i, y_i\})} = Tr [M(r_{N_\tau}) \cdots M(r_1)]. \quad (89)$$

Using this property, the path integral representation of integrated particle propagator is simplified to,

$$\frac{C(\tau)}{C_0(\tau)} = \int \prod_{i=1}^{N_\tau} dr_i \frac{e^{-S_E^{(\omega)}(\{r_i\})} Tr [M(r_{N_\tau}) \cdots M(r_1)]}{C_0(\tau)}. \quad (90)$$

This expression is reminiscent of path integrals in lattice QCD after fermion degrees of freedom are integrated out, with  $Tr[\cdots]$  serving as ‘fermion loops’. It can be evaluated by Monte Carlo importance sampling,

$$\frac{C(\tau)}{C_0(\tau)} = \frac{1}{N_{cfg}} \sum_{\alpha=1}^{N_{cfg}} \frac{Tr [M(r_{N_\tau}^{(\alpha)}) \cdots M(r_1^{(\alpha)})]}{e^{-\sigma_1 \tau} + e^{-\sigma_2 \tau}}, \quad (91)$$

where  $N_{cfg}$  is the total number of configurations. The random values of  $\{r_i^{(\alpha)}\}$  for the  $\alpha$ -th configuration are generated according to the harmonic oscillator trap probability density distribution:

$$p^{(\omega)}(\{r_i\}) = \frac{e^{-S_E^{(\omega)}(\{r_i\})}}{\int \prod_{i=1}^{N_\tau} dr_i e^{-S_E^{(\omega)}(\{r_i\})}}. \quad (92)$$

If we define the coupled-channel propagation amplitudes matrix in Minkowski time by,

$$U(r, r'; t) \stackrel{t=-i\tau}{=} \int \prod_{i=1}^{N_\tau-1} dr_i e^{-S_E^{(\omega)}(\{r_i\})} M(r_{N_\tau-1}) \cdots M(r_1), \quad (93)$$

then in the continuum limit of  $a_\tau \rightarrow 0$ , the  $U$  matrix satisfies coupled-channel Schrödinger equation,

$$i \frac{\partial U(r, r'; t)}{\partial t} = \left( \begin{bmatrix} H_r^{(\omega)} & 0 \\ 0 & H_r^{(\omega)} \end{bmatrix} + V(r) \right) U(r, r'; t), \quad (94)$$

where  $r \neq r'$ , and the potential matrix approaches,

$$V(r) = -\frac{1}{a_\tau} \ln M(r) \xrightarrow{a_\tau \rightarrow 0} \begin{bmatrix} \sigma_1 + V_1(r) & \gamma(r) \\ \gamma(r) & \sigma_2 + V_2(r) \end{bmatrix}. \quad (95)$$

The total Hamiltonian matrix at continuum limit then takes the form,

$$\hat{H}^{(trap)} = \begin{bmatrix} \sigma_1 + H_r^{(\omega)} + V_1(r) & \gamma(r) \\ \gamma(r) & \sigma_2 + H_r^{(\omega)} + V_2(r) \end{bmatrix}, \quad (96)$$

which indeed describes a coupled-channel system in a harmonic oscillator trap.

### C. Monte Carlo simulation of coupled-channel system vs. exact solution vs. infinite volume limit

In this subsection, we carry out Monte Carlo sampling calculation of  $\frac{C(\tau)}{C_0(\tau)}$  defined in Eq.(91) with two different traps in  $y$ -direction: a harmonic trap or a hard wall trap.

In both cases, two lowest even-parity states are installed in the density matrix. Since the eigenstates are analytical in both cases, they lead to exact effective potentials in  $r$ -direction, which offers a way to check the Monte Carlo. For harmonic oscillator trap with angular frequency  $\omega_y$ ,

$$\begin{aligned}\chi_1(y) &= \left(\frac{m\omega_y}{\pi}\right)^{\frac{1}{4}} e^{-\frac{m\omega_y}{2}y^2} H_0(\sqrt{m\omega_y}y), \quad \sigma_1 = \frac{\omega_y}{2}, \\ \chi_2(y) &= \frac{1}{\sqrt{2^3}} \left(\frac{m\omega_y}{\pi}\right)^{\frac{1}{4}} e^{-\frac{m\omega_y}{2}y^2} H_2(\sqrt{m\omega_y}y), \quad \sigma_2 = \frac{5\omega_y}{2}.\end{aligned}\quad (97)$$

For hard-wall trap with walls placed at the two boundaries  $y = 0$  and  $y = L_y$ ,

$$\begin{aligned}\chi_1(y) &= \sqrt{\frac{2}{L_y}} \sin \frac{\pi y}{L_y}, \quad \sigma_1 = \frac{\pi^2}{2mL_y^2}, \\ \chi_2(y) &= \sqrt{\frac{2}{L_y}} \sin \frac{3\pi y}{L_y}, \quad \sigma_2 = \frac{9\pi^2}{2mL_y^2}.\end{aligned}\quad (98)$$

The quasi-1D coupled-channel effective potentials have square-well shape:

$$\begin{aligned}V_n(r) &= \begin{cases} \frac{V_n}{b}, & \text{if } r \in [-\frac{b}{2}, \frac{b}{2}], \\ 0, & \text{otherwise,} \end{cases}, \quad n = 1, 2, \\ \gamma(r) &= \begin{cases} \frac{\gamma}{b}, & \text{if } r \in [-\frac{b}{2}, \frac{b}{2}], \\ 0, & \text{otherwise.} \end{cases}\end{aligned}\quad (99)$$

The strengths of the square well potentials are given by

$$\begin{aligned}V_n &= -\frac{b}{a_\tau} \ln \left[ 1 + \kappa_n \left( e^{-\frac{a_\tau V_0}{bb_y}} - 1 \right) \right], \quad n = 1, 2, \\ \gamma &= -\frac{b}{a_\tau} \kappa_\gamma \left( e^{-\frac{a_\tau V_0}{bb_y}} - 1 \right),\end{aligned}\quad (100)$$

where the  $\kappa$  parameters are, for harmonic oscillator trap ( $y_0 = 0$ ),

$$\begin{aligned}\kappa_1 &= \operatorname{erf}\left(\frac{\sqrt{m\omega_y b_y^2}}{2}\right), \\ \kappa_2 &= \operatorname{erf}\left(\frac{\sqrt{m\omega_y b_y^2}}{2}\right) - \frac{2 + m\omega_y b_y^2}{4} \sqrt{\frac{m\omega_y b_y^2}{\pi}} e^{-\frac{m\omega_y b_y^2}{4}}, \\ \kappa_\gamma &= -\sqrt{\frac{m\omega_y b_y^2}{2\pi}} e^{-\frac{m\omega_y b_y^2}{4}};\end{aligned}\quad (101)$$

and for hard wall trap ( $y_0 = \frac{L_y}{2}$ ),

$$\begin{aligned}\kappa_1 &= \frac{b_y}{L_y} + \frac{1}{\pi} \sin \frac{\pi b_y}{L_y}, \\ \kappa_2 &= \frac{b_y}{L_y} + \frac{1}{3\pi} \sin \frac{3\pi b_y}{L_y}, \\ \kappa_\gamma &= -\frac{1 + \cos \frac{\pi b_y}{L_y}}{\pi} \sin \frac{\pi b_y}{L_y}.\end{aligned}\quad (102)$$

With all the ingredients in place, we are ready to make a detailed comparison in the quasi-one-dimensional model for coupled-channel dynamics from three perspectives.

First, the Monte Carlo simulation of  $\frac{C(\tau)}{C_0(\tau)}$  in Eq.(91) for quasi-1D coupled-channel systems in a harmonic oscillator trap along  $r$ -direction can be carried out by either standard Metropolis algorithm [70, 71] or Hybrid Monte Carlo (HMC) algorithm [72] (HMC is used in this work). The Monte Carlo sampling configurations for non-interacting particles in a harmonic oscillator trap are generated according to Eq.(92). The simulation is performed with fixed lattice spacing  $a_\tau \sim 0.04$ , so the number of steps in temporal dimension,  $N_\tau$  varies for  $\tau \in [0.5, 5.5]$ . Typically a half million measurements are generated for each  $\tau$ . The choice of other parameters are  $V_0 = 1$ ,  $m = 1$  and  $b = b_y = 0.2$  for a square well potential. Three different sizes ( $\omega = 0.1, 0.2$  and  $0.5$ ) are used for the harmonic oscillator trap in  $r$ -direction.

Second, the energy spectrum  $\{E_l\}$  of quasi-1D coupled-channel systems in a harmonic oscillator trap interacting with square well potentials defined in Eq.(99) and Eq.(100) can be obtained by diagonalizing the Hamiltonian in Eq.(57), where the matrix elements are evaluated by

$$\begin{aligned}V_{l,l'}^{(n)} &= V_n \int_{-\frac{b}{2}}^{\frac{b}{2}} dr \phi_l(r) \phi_{l'}(r), \quad n = 1, 2, \\ \gamma_{l,l'} &= \gamma \int_{-\frac{b}{2}}^{\frac{b}{2}} dr \phi_l(r) \phi_{l'}(r),\end{aligned}\quad (103)$$

using the harmonic oscillator basis in Eq.(56). The exact solution of  $\frac{C(\tau)}{C_0(\tau)}$  can then be obtained by feeding  $\{E_l\}$  to  $C(\tau)$  in Eq.(58), and using  $C_0(\tau)$  in Eq.(59).

Third, the scattering solutions in infinite volume can be well approximated by contact interactions for small  $b$ . The analytic expression of phase shifts and inelasticity for contact interaction potentials are given in Eq.(52) and Eq.(55). At infinite volume limit,

$$\frac{C(\tau)}{C_0(\tau)} \xrightarrow{\omega \rightarrow 0} 1 + \frac{1}{C_0(\tau)} \frac{\tau}{\pi} \left[ \int_{\sigma_1}^{\infty} \delta_1(\epsilon) + \int_{\sigma_2}^{\infty} \delta_2(\epsilon) \right] e^{-\epsilon\tau} d\epsilon.\quad (104)$$

It is basically Eq.(31) in a harmonic trap recast in ratio form for comparison purposes.

In Fig. 4 we show the comparison for the three sizes of harmonic oscillator trap in  $r$ -direction and harmonic oscillator trap in  $y$ -direction with parameters of  $\omega_y = 0.2$  and  $y_0 = 0$ . The same is shown in Fig. 5 for hard wall trap in  $y$ -direction with parameters of  $L_y = 4$  and  $y_0 = 2$ . We see that the Monte Carlo results are in excellent agreement with the exact solutions, and they both approach their infinite volume limit rapidly as the size of trap in  $r$ -direction is widened ( $\omega \rightarrow 0$ ). Moreover, the agreement is insensitive to the type of traps used in  $y$ -direction. Validated by exact solutions, the Monte Carlo

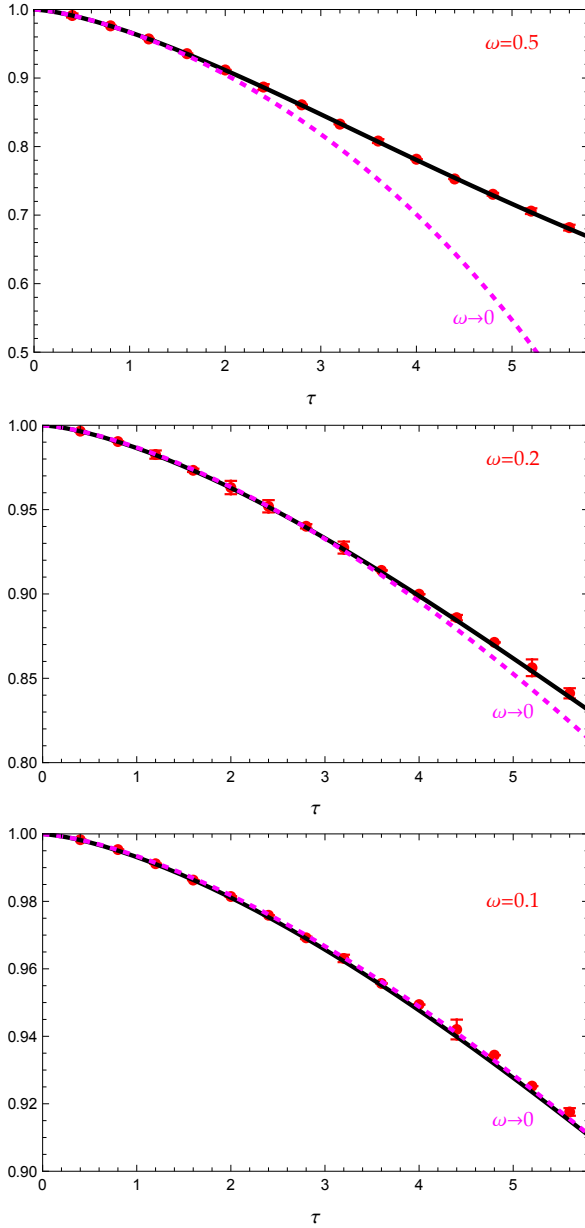


FIG. 4: Convergence check of Eq.(104) for **harmonic oscillator** trap placed in  $y$ -direction. The three graphs correspond to harmonic oscillator trap size  $\omega = 0.1, 0.2, 0.5$  in  $r$ -direction. The red points with error bars are Monte Carlo data of  $\frac{C(\tau)}{C_0(\tau)}$  on the left-hand-side. The solid black curves are exact results for  $\frac{C(\tau)}{C_0(\tau)}$  from energy spectrum representation. The dashed purple curves are the infinite volume limit on the right-hand-side. Other parameters are taken as:  $V_0 = 5$ ,  $b = 0.2$ ,  $a_\tau = 0.04$ ,  $m = 1$ ,  $\sigma_1 = 0.1$ , and  $\sigma_2 = 0.5$ . The effective potential strengths are  $V_1 = 0.257$ ,  $V_2 = 0.126$ , and  $\gamma = -0.177$ .

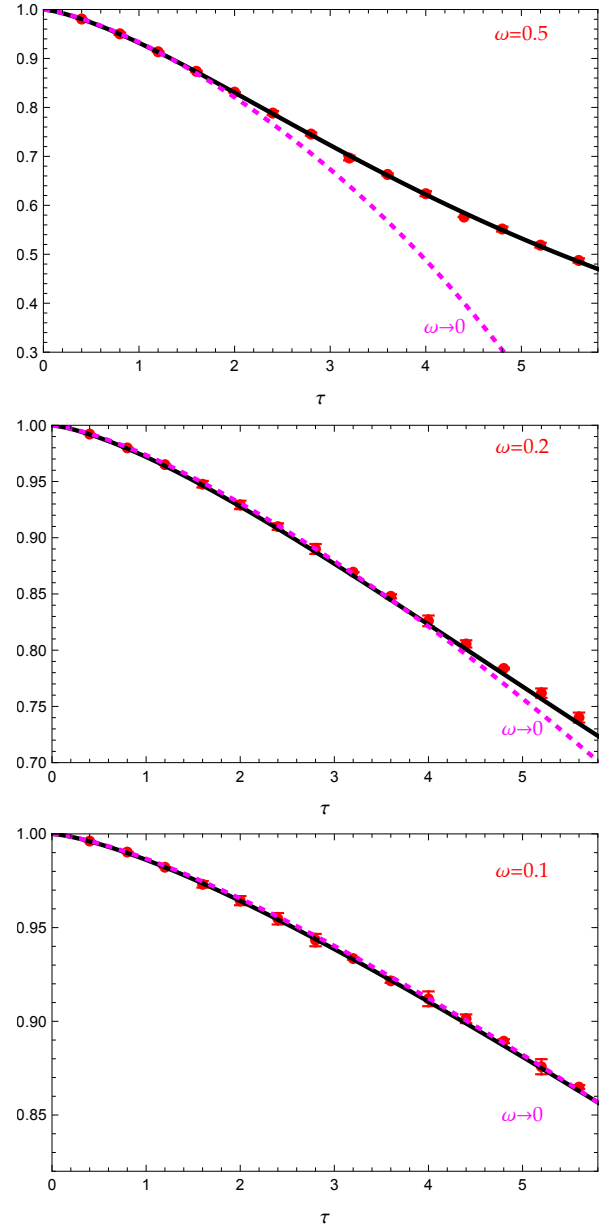


FIG. 5: Similar to Fig. 4 but for **hard-wall** trap placed in  $y$ -direction with parameters  $L_y = 4$ ,  $y_0 = 2.0$  and  $b_y = 0.2$ . Other parameters are taken as:  $V_0 = 5$ ,  $b = 0.2$ ,  $a_\tau = 0.04$ ,  $m = 1$ ,  $\sigma_1 = 0.31$ , and  $\sigma_2 = 2.77$ . The effective potential strengths are  $V_1 = 0.522$ ,  $V_2 = 0.513$ , and  $\gamma = -0.492$ .

approach can serve as a general method to the coupled-channel formalism where general interaction and trap potentials can be used.

## V. SUMMARY AND OUTLOOK

In this work, we extended the integrated correlation function formalism developed in Refs. [1, 2] from single channel to two coupled channels. The central result in Euclidean space is represented by Eq.(31). Remarkably, it bears the same structure as the single-channel result in Eq.(2): just from a single phase shift term to sum of two phase shift terms with appropriate thresholds on the right hand side. Both relations are reproduced here for a side-by-side comparison.

### Single channel:

$$C(\tau) - C_0(\tau) \xrightarrow{\text{trap} \rightarrow \infty} \frac{\tau}{\pi} \int_0^\infty d\epsilon \delta(\epsilon) e^{-\epsilon\tau}.$$

### Two coupled channels:

$$C(\tau) - C_0(\tau) \xrightarrow{\text{trap} \rightarrow \infty} \frac{\tau}{\pi} \left[ \int_{\sigma_1}^\infty \delta_1(\epsilon) + \int_{\sigma_2}^\infty \delta_2(\epsilon) \right] e^{-\epsilon\tau} d\epsilon.$$

In this formalism, the difference of integrated correlation functions between interacting and non-interacting systems in a trap is related to the infinite-volume phase shifts by a weighted integral over energy. It can be regarded as an alternative method to the well-known Lüscher formula. The new relation is validated in a number of ways, including exactly solvable models and Monte Carlo simulation that can admit general interaction potentials. Several comments are in order.

1. The relation has two salient features. One is the rapid convergence to the infinite-volume limit at short times as the trap size is increased. The other is that it involves directly correlation functions, bypassing the requirement to extract energy spectrum in traditional methods. Both features bode well for application in lattice QCD simulations to overcome signal-to-noise and energy level density issues often encountered in baryon systems as the volume is increased.
2. Given the integrated correlation functions, we only have one constraint for two phase shifts via the relation. The situation is similar to the coupled-channel Lüscher and BERW formulism, see e.g. Refs.[10, 11, 61], where the quantization condition involves two phase shifts and one inelasticity. One strategy of extracting coupled-channel dynamics is to model the system based on chiral perturbation theory or dispersion relation with a few free parameters, so that the explicit dependence on these parameters and expressions for the phase shifts and inelasticity are available. By fitting the two phase shifts to the integrated correlated

function data, the free parameters of the model may be determined, which in turn yields the inelasticity. Alternatively, extra constraints may be obtained by defining the correlation functions in each individual channel. This discussion is detailed in Appendix A.

3. Although developed for two coupled channels, the relation straightforwardly carries over to more than two channels,

$$C(\tau) - C_0(\tau) \xrightarrow{\text{trap} \rightarrow \infty} \frac{\tau}{\pi} \sum_{n>2} \int_{\sigma_n}^\infty \delta_n(\epsilon) e^{-\epsilon\tau} d\epsilon. \quad (105)$$

The reason is that the coupled-channel relation is only explicitly related to phase shifts, not inelasticity ( $\eta$ ). The key observation is that the integrated correlation function of coupled-channel systems in infinite volume is defined through the trace of full Green's function matrix, see Eq.(20). For multi-channel systems, the trace of Green's function is related to the determinant of  $S$ -matrix [58] by,

$$\text{Tr} \left[ \mathcal{G}^{(\infty)}(E) - \mathcal{G}_0^{(\infty)}(E) \right] = -\frac{1}{\pi} \int_0^\infty d\lambda \frac{\frac{1}{2i} \ln \det [S(\lambda)]}{(\lambda - E)^2}, \quad (106)$$

where the determinant is only explicitly dependent on the phase shifts,

$$\det [S(\lambda)] = e^{2i \sum_n \delta_n(\lambda)}. \quad (107)$$

The inelasticities are implicitly present in the formalism.

4. We envision no issues in extending the formalism to relativistic dynamics as demonstrated in the single-channel case [2].
5. The trap in the formalism refers to any potential that can confine the system to have quantized energy levels. The common choices are harmonic oscillator trap, hard-wall trap, periodic box of size  $L$ , or periodic lattices of size  $N$  and spacing  $a$  that extrapolate to  $\lim_{\substack{N \rightarrow \infty \\ a \rightarrow 0}} Na = L$ . Future work would benefit from applying the formalism in more practical scenarios. One possible avenue is to build on the  $\phi^4$  lattice model in Ref.[2] to go from 1+1 dimensions to 3+1 dimensions. Such a demonstration can inform us on the convergence rate and computational demand in Monte Carlo simulations of lattice field theories.

## ACKNOWLEDGMENTS

This research is supported in part by the U.S. National Science Foundation under Grant No. NSF PHY-2418937 (P.G.) and NSF PHY-1748958 (P.G.), and the U.S. Department of Energy under Grant No. DE-FG02-95ER40907 (F.L.).

- 
- [1] P. Guo and V. Gasparian, Toward extracting the scattering phase shift from integrated correlation functions, *Phys. Rev. D* **108**, 074504 (2023), arXiv:2307.12951 [hep-lat].
- [2] P. Guo, Toward extracting the scattering phase shift from integrated correlation functions. II. A relativistic lattice field theory model, *Phys. Rev. D* **110**, 014504 (2024), arXiv:2402.15628 [hep-lat].
- [3] M. Lüscher, Two particle states on a torus and their relation to the scattering matrix, *Nucl.Phys.* **B354**, 531 (1991).
- [4] K. Rummukainen and S. A. Gottlieb, Resonance scattering phase shifts on a nonrest frame lattice, *Nucl. Phys.* **B450**, 397 (1995), arXiv:hep-lat/9503028 [hep-lat].
- [5] N. H. Christ, C. Kim, and T. Yamazaki, Finite volume corrections to the two-particle decay of states with non-zero momentum, *Phys. Rev.* **D72**, 114506 (2005), arXiv:hep-lat/0507009 [hep-lat].
- [6] V. Bernard, M. Lage, U.-G. Meißner, and A. Rusetsky, Resonance properties from the finite-volume energy spectrum, *JHEP* **08**, 024, arXiv:0806.4495 [hep-lat].
- [7] S. He, X. Feng, and C. Liu, Two particle states and the S-matrix elements in multi-channel scattering, *JHEP* **07**, 011, arXiv:hep-lat/0504019.
- [8] M. Lage, U.-G. Meißner, and A. Rusetsky, A Method to measure the antikaon-nucleon scattering length in lattice QCD, *Phys. Lett.* **B681**, 439 (2009), arXiv:0905.0069 [hep-lat].
- [9] M. Döring, U.-G. Meißner, E. Oset, and A. Rusetsky, Unitarized Chiral Perturbation Theory in a finite volume: Scalar meson sector, *Eur. Phys. J.* **A47**, 139 (2011), arXiv:1107.3988 [hep-lat].
- [10] P. Guo, J. Dudek, R. Edwards, and A. P. Szczepaniak, Coupled-channel scattering on a torus, *Phys. Rev.* **D88**, 014501 (2013), arXiv:1211.0929 [hep-lat].
- [11] P. Guo, Coupled-channel scattering in 1+1 dimensional lattice model, *Phys. Rev.* **D88**, 014507 (2013), arXiv:1304.7812 [hep-lat].
- [12] S. Kreuzer and H. W. Hammer, Efimov physics in a finite volume, *Phys. Lett.* **B673**, 260 (2009), arXiv:0811.0159 [nucl-th].
- [13] K. Polejaeva and A. Rusetsky, Three particles in a finite volume, *Eur. Phys. J.* **A48**, 67 (2012), arXiv:1203.1241 [hep-lat].
- [14] M. T. Hansen and S. R. Sharpe, Relativistic, model-independent, three-particle quantization condition, *Phys. Rev.* **D90**, 116003 (2014), arXiv:1408.5933 [hep-lat].
- [15] M. Mai and M. Döring, Three-body Unitarity in the Finite Volume, *Eur. Phys. J.* **A53**, 240 (2017), arXiv:1709.08222 [hep-lat].
- [16] M. Mai and M. Döring, Finite-Volume Spectrum of  $\pi^+\pi^+$  and  $\pi^+\pi^+\pi^+$  Systems, *Phys. Rev. Lett.* **122**, 062503 (2019), arXiv:1807.04746 [hep-lat].
- [17] M. Döring, H. W. Hammer, M. Mai, J. Y. Pang, A. Rusetsky, and J. Wu, Three-body spectrum in a finite volume: the role of cubic symmetry, *Phys. Rev.* **D97**, 114508 (2018), arXiv:1802.03362 [hep-lat].
- [18] P. Guo, One spatial dimensional finite volume three-body interaction for a short-range potential, *Phys. Rev.* **D95**, 054508 (2017), arXiv:1607.03184 [hep-lat].
- [19] P. Guo and V. Gasparian, An solvable three-body model in finite volume, *Phys. Lett.* **B774**, 441 (2017), arXiv:1701.00438 [hep-lat].
- [20] P. Guo and V. Gasparian, Numerical approach for finite volume three-body interaction, *Phys. Rev.* **D97**, 014504 (2018), arXiv:1709.08255 [hep-lat].
- [21] P. Guo and T. Morris, Multiple-particle interaction in (1+1)-dimensional lattice model, *Phys. Rev.* **D99**, 014501 (2019), arXiv:1808.07397 [hep-lat].
- [22] M. Mai, M. Döring, C. Culver, and A. Alexandru, Three-body unitarity versus finite-volume  $\pi^+\pi^+\pi^+$  spectrum from lattice QCD, *Phys. Rev. D* **101**, 054510 (2020), arXiv:1909.05749 [hep-lat].
- [23] P. Guo, Threshold expansion formula of  $N$  bosons in a finite volume from a variational approach, *Phys. Rev. D* **101**, 054512 (2020), arXiv:2002.04111 [hep-lat].
- [24] P. Guo, M. Döring, and A. P. Szczepaniak, Variational approach to  $N$ -body interactions in finite volume, *Phys. Rev.* **D98**, 094502 (2018), arXiv:1810.01261 [hep-lat].
- [25] P. Guo, Propagation of particles on a torus, *Phys. Lett. B* **804**, 135370 (2020), arXiv:1908.08081 [hep-lat].
- [26] P. Guo and M. Döring, Lattice model of heavy-light three-body system, *Phys. Rev. D* **101**, 034501 (2020), arXiv:1910.08624 [hep-lat].
- [27] P. Guo and B. Long, Multi- $\pi^+$  systems in a finite volume, *Phys. Rev. D* **101**, 094510 (2020), arXiv:2002.09266 [hep-lat].
- [28] P. Guo, Modeling few-body resonances in finite volume, *Phys. Rev. D* **102**, 054514 (2020), arXiv:2007.12790 [hep-lat].
- [29] A. J. Woss, D. J. Wilson, and J. J. Dudek, Efficient solution of the multichannel lüscher determinant condition through eigenvalue decomposition, *Physical Review D* **101**, 10.1103/physrevd.101.114505 (2020).
- [30] M. Fischer, B. Kostrzewa, L. Liu, F. Romero-López, M. Ueding, and C. Urbach, Scattering of two and three physical pions at maximal isospin from lattice QCD, *Eur. Phys. J. C* **81**, 436 (2021), arXiv:2008.03035 [hep-lat].
- [31] M. T. Hansen, R. A. Briceño, R. G. Edwards, C. E. Thomas, and D. J. Wilson (Hadron Spectrum), Energy-Dependent  $\pi^+\pi^+\pi^+$  Scattering Amplitude from QCD, *Phys. Rev. Lett.* **126**, 012001 (2021), arXiv:2009.04931 [hep-lat].
- [32] T. D. Blanton, A. D. Hanlon, B. Hörz, C. Morningstar, F. Romero-López, and S. R. Sharpe, Interactions of two and three mesons including higher partial waves from lattice qcd (2021), arXiv:2106.05590 [hep-lat].
- [33] M. Mai, A. Alexandru, R. Brett, C. Culver, M. Döring, F. X. Lee, and D. Sadasivan, Three-body dynamics of the  $a_1(1260)$  resonance from lattice qcd (2021), arXiv:2107.03973 [hep-lat].
- [34] L. Bovermann, E. Epelbaum, H. Krebs, and D. Lee, Scattering phase shifts and mixing angles for an arbitrary number of coupled channels on the lattice, *Physical Review C* **100**, 10.1103/physrevc.100.064001 (2019).
- [35] F. X. Lee, C. Morningstar, and A. Alexandru, Energy spectrum of two-particle scattering in a periodic box, *Int. J. Mod. Phys. C* **31**, 2050131 (2020).
- [36] D. Guo, A. Alexandru, R. Molina, M. Mai, and M. Döring, Extraction of isoscalar  $\pi\pi$  phase-shifts from lattice QCD, *Phys. Rev.* **D98**, 014507 (2018),



- arXiv:1803.02897 [hep-lat].
- [37] C. Culver, M. Mai, A. Alexandru, M. Döring, and F. X. Lee, Pion scattering in the isospin  $I = 2$  channel from elongated lattices, *Phys. Rev. D* **100**, 034509 (2019), arXiv:1905.10202 [hep-lat].
- [38] A. Alexandru, R. Brett, C. Culver, M. Döring, D. Guo, F. X. Lee, and M. Mai, Finite-volume energy spectrum of the  $K^- K^- K^-$  system, *Phys. Rev. D* **102**, 114523 (2020), arXiv:2009.12358 [hep-lat].
- [39] R. Brett, C. Culver, M. Mai, A. Alexandru, M. Döring, and F. X. Lee, Three-body interactions from the finite-volume QCD spectrum, *Phys. Rev. D* **104**, 014501 (2021), arXiv:2101.06144 [hep-lat].
- [40] R. A. Briceño, J. J. Dudek, R. G. Edwards, and D. J. Wilson, Isoscalar  $\pi\pi$  scattering and the  $\sigma$  meson resonance from QCD, *Phys. Rev. Lett.* **118**, 022002 (2017), arXiv:1607.05900 [hep-ph].
- [41] G. Moir, M. Peardon, S. M. Ryan, C. E. Thomas, and D. J. Wilson, Coupled-Channel  $D\pi$ ,  $D\eta$  and  $D_s\bar{K}$  Scattering from Lattice QCD, *JHEP* **10**, 011, arXiv:1607.07093 [hep-lat].
- [42] M. Mai, M. Döring, and A. Rusetsky, Multi-particle systems on the lattice and chiral extrapolations: a brief review, *Eur. Phys. J. ST* **230**, 1623 (2021), arXiv:2103.00577 [hep-lat].
- [43] A. Rusetsky, Three particles on the lattice, *PoS LATTICE2019*, 281 (2019), arXiv:1911.01253 [hep-lat].
- [44] M. Mai, A. Alexandru, R. Brett, C. Culver, M. Döring, F. X. Lee, and D. Sadasivan (GWQCD), Three-Body Dynamics of the  $a_1(1260)$  Resonance from Lattice QCD, *Phys. Rev. Lett.* **127**, 222001 (2021), arXiv:2107.03973 [hep-lat].
- [45] F. X. Lee, A. Alexandru, and R. Brett, Validation of the finite-volume quantization condition for two spinless particles, *Phys. Rev. D* **105**, 054517 (2022), arXiv:2107.04430 [hep-lat].
- [46] N. Ishii, S. Aoki, and T. Hatsuda, Nuclear force from lattice qcd, *Phys. Rev. Lett.* **99**, 022001 (2007).
- [47] S. Aoki, T. Hatsuda, and N. Ishii, Theoretical Foundation of the Nuclear Force in QCD and Its Applications to Central and Tensor Forces in Quenched Lattice QCD Simulations, *Progress of Theoretical Physics* **123**, 89 (2010), <https://academic.oup.com/ptp/article-pdf/123/1/89/9681302/123-1-89.pdf>.
- [48] T. Iritani, S. Aoki, T. Doi, S. Gongyo, T. Hatsuda, Y. Ikeda, T. Inoue, N. Ishii, H. Nemura, and K. Sasaki (HAL QCD Collaboration), Systematics of the  $hal$  qcd potential at low energies in lattice qcd, *Phys. Rev. D* **99**, 014514 (2019).
- [49] N. Ishii, S. Aoki, T. Doi, T. Hatsuda, Y. Ikeda, T. Inoue, K. Murano, H. Nemura, and K. Sasaki, Hadron-hadron interactions from imaginary-time nambu-bethe-salpeter wave function on the lattice, *Physics Letters B* **712**, 437 (2012).
- [50] S. Aoki, Nucleon-nucleon interactions via lattice qcd: Methodology, *The European Physical Journal A* **49**, 81 (2013).
- [51] G. P. Lepage, The analysis of algorithms for lattice field theory, *Boulder ASI* **1989**, 97 (1989).
- [52] C. Drischler, W. Haxton, K. McElvain, E. Mereghetti, A. Nicholson, P. Vranas, and A. Walker-Loud, Towards grounding nuclear physics in qcd, *Progress in Particle and Nuclear Physics* **121**, 103888 (2021).
- [53] J. Bulava and M. T. Hansen, Scattering amplitudes from finite-volume spectral functions, *Phys. Rev. D* **100**, 034521 (2019), arXiv:1903.11735 [hep-lat].
- [54] S. Aoki and T. Doi, Lattice qcd and baryon-baryon interactions, in *Handbook of Nuclear Physics*, edited by I. Tanihata, H. Toki, and T. Kajino (Springer Nature Singapore, Singapore, 2020) pp. 1–31.
- [55] M. Hansen, A. Lupo, and N. Tantalo, Extraction of spectral densities from lattice correlators, *Phys. Rev. D* **99**, 094508 (2019), arXiv:1903.06476 [hep-lat].
- [56] G. Bailas, S. Hashimoto, and T. Ishikawa, Reconstruction of smeared spectral function from Euclidean correlation functions, *PTEP* **2020**, 043B07 (2020), arXiv:2001.11779 [hep-lat].
- [57] P. Guo and V. Gasparian, Friedel formula and Krein's theorem in complex potential scattering theory, *Phys. Rev. Res.* **4**, 023083 (2022), arXiv:2202.12465 [cond-mat.other].
- [58] P. Guo, V. Gasparian, A. Pérez-Garrido, and E. Jódar, Tunneling time in coupled-channel systems, *Phys. Rev. Res.* **6**, 043032 (2024), arXiv:2407.17981 [cond-mat.other].
- [59] P. Guo, R. Mitchell, and A. P. Szczepaniak, The Role of P-wave inelasticity in  $J/\psi \rightarrow \pi^+ \pi^- \pi^0$ , *Phys. Rev. D* **82**, 094002 (2010), arXiv:1006.4371 [hep-ph].
- [60] P. Guo, R. Mitchell, M. Shepherd, and A. P. Szczepaniak, Amplitudes for the analysis of the decay  $J/\psi \rightarrow K^+ K^- \pi^0$ , *Phys. Rev. D* **85**, 056003 (2012), arXiv:1112.3284 [hep-ph].
- [61] P. Guo and B. Long, Nuclear reactions in artificial traps, *J. Phys. G* **49**, 055104 (2022), arXiv:2101.03901 [nucl-th].
- [62] M. S. Birman and M. G. Krein, On the theory of wave operators and scattering operators, *Sov. Math., Dokl.* **3**, 740 (1962).
- [63] J. Friedel, Electronic structure of primary solid solutions in metals, *Advances in Physics* **3**, 446 (1954), <https://doi.org/10.1080/00018735400101233>.
- [64] J. Friedel, Metallic alloys, *Il Nuovo Cimento* (1955-1965) **7**, 287 (1958).
- [65] J. S. Faulkner, Scattering theory and cluster calculations, *Journal of Physics C: Solid State Physics* **10**, 4661 (1977).
- [66] P. Guo and V. Gasparian, Charged particles interaction in both a finite volume and a uniform magnetic field, *Phys. Rev. D* **103**, 094520 (2021), arXiv:2101.01150 [hep-lat].
- [67] P. Guo, Coulomb corrections to two-particle interactions in artificial traps, *Phys. Rev. C* **103**, 064611 (2021), arXiv:2101.11097 [nucl-th].
- [68] P. Guo and B. Long, Visualizing resonances in finite volume, *Phys. Rev. D* **102**, 074508 (2020), arXiv:2007.10895 [hep-lat].
- [69] T. Busch, B.-G. Englert, K. Rzazewski, and M. Wilkens, Two Cold Atoms in a Harmonic Trap, *Found. Phys.* **28**, 549–559 (1998).
- [70] M. Creutz and B. Freedman, A STATISTICAL APPROACH TO QUANTUM MECHANICS, *Annals Phys.* **132**, 427 (1981).
- [71] G. P. Lepage, Lattice QCD for novices, in *13th Annual HUGS AT CEBAF (HUGS 98)* (1998) pp. 49–90, arXiv:hep-lat/0506036.
- [72] S. Duane, A. Kennedy, B. J. Pendleton, and D. Roweth, Hybrid monte carlo, *Physics Letters B* **195**, 216 (1987).



### Appendix A: Inelastic effect in individual channel of a coupled-channel system

The inelastic effect in total integrated correlation functions by summing over the contribution from both channels is not explicitly present in Eq.(31) via inelasticity. As discussed in Ref. [58], the imaginary part of the trace of integrated Green's function is related to the determinant of  $S$ -matrix by

$$\text{Im} \left[ \text{Tr} \left[ G^{(\infty)}(\lambda) - G_0^{(\infty)}(\lambda) \right] \right] = -\frac{1}{2i} \frac{d}{d\lambda} \ln \det [S(\lambda)], \quad (\text{A1})$$

where

$$\det [S(\lambda)] = e^{2i[\delta_1(\lambda) + \delta_2(\lambda)]}. \quad (\text{A2})$$

The inelasticity is canceled out in determinant of  $S$ -matrix, which is warranted by the Friedel formula, see e.g. Refs. [57, 65]. We show in the following that the explicit dependence of inelasticity shows up in each individual channel integrated correlation functions.

As illustrated in Ref. [58], for each individual channel, the diagonal terms of infinite volume integrated Green's function for coupled-channel systems are

$$\begin{aligned} & \int_{-\infty}^{\infty} dr \left[ G_{nn}^{(\infty)}(r, r; E) - G_n^{(\infty,0)}(0; E) \right] \\ &= -\frac{\mu_n}{k_n} \frac{\partial}{\partial k_n} \ln t_{nn}(k_1, k_2), \end{aligned} \quad (\text{A3})$$

where  $t_{nn}(k_1, k_2)$  denote diagonal terms of transmission amplitude that are defined via diagonal scattering amplitudes by

$$t_{nn}(k_1, k_2) = 1 + i \frac{\mu_n}{k_n} T_{nn} = \frac{\eta e^{2i\delta_n} + 1}{2}. \quad (\text{A4})$$

Notation-wise, the dependent on  $(k_1, k_2)$  in  $t_{nn}(k_1, k_2)$  is written explicitly to remind readers that the diagonal term of integrated Green's function is related to corresponding transmission amplitude by partial derivative. We also find

$$\text{Im} \int_{-\infty}^{\infty} dr \left[ G_{nn}^{(\infty)}(r, r; E) - G_n^{(\infty,0)}(0; E) \right] = -\frac{\mu_n}{k_n} \frac{\partial \Phi_n(E)}{\partial k_n}, \quad (\text{A5})$$

where  $\Phi_n(E)$  is the phase of  $t_{nn}(k_1, k_2)$ :

$$\Phi_n(E) = \tan^{-1} \frac{\text{Im}[t_{nn}(k_1, k_2)]}{\text{Re}[t_{nn}(k_1, k_2)]} = \tan^{-1} \left[ \frac{\eta \sin(2\delta_n)}{\eta \cos(2\delta_n) + 1} \right]. \quad (\text{A6})$$

At the elastic limit by turning off coupling  $\eta \rightarrow 1$ ,  $\Phi_n(E)$  is reduced to the elastic scattering phase shift  $\delta_n(E)$ . Let's define a extra phase factor by

$$\Delta_n(E) = \delta_n(\sigma_n) + \int_{\sigma_n}^E d\lambda \frac{\mu_n}{k_n(\lambda)} \frac{\partial \Phi_n(\lambda)}{\partial k_n(\lambda)}, \quad (\text{A7})$$

so that

$$\frac{d\Delta_n(E)}{dE} = \frac{\mu_n}{k_n} \frac{\partial \Phi_n(E)}{\partial k_n}, \quad (\text{A8})$$

hence Eq.(A5) can be written as

$$\text{Im} \int_{-\infty}^{\infty} dr \left[ G_{nn}^{(\infty)}(r, r; E) - G_n^{(\infty,0)}(0; E) \right] = -\frac{d\Delta_n(E)}{dE}. \quad (\text{A9})$$

Using the analytical properties of Green's function, Eq.(A3) is thus given in terms of  $\Delta_n(E)$  by

$$\begin{aligned} & \int_{-\infty}^{\infty} dr \left[ G_{nn}^{(\infty)}(r, r; E) - G_n^{(\infty,0)}(0; E) \right] \\ &= -\frac{1}{\pi} \int_{\sigma_n}^{\infty} d\lambda \frac{\Delta_n(\lambda)}{(\lambda - E)^2}. \end{aligned} \quad (\text{A10})$$

Therefore we find

$$\begin{aligned} & \int_{-\infty}^{\infty} \frac{d\lambda}{2\pi} \int_{-\infty}^{\infty} dr \left[ G_{nn}^{(\infty)}(r, r; E) - G_n^{(\infty,0)}(0; E) \right] e^{-i\lambda t} \\ &= \frac{t}{\pi} \int_{\sigma_n}^{\infty} d\epsilon \Delta_n(\epsilon) e^{-i\epsilon t}. \end{aligned} \quad (\text{A11})$$

Comparing Eq.(29) with Eq.(A9), we obtain

$$\sum_{i=1}^2 \frac{d\Delta_n(E)}{dE} = \frac{d[\delta_1(E) + \delta_2(E)]}{dE}. \quad (\text{A12})$$

In fact, with some tedious calculation and using relations given in Ref. [58], we can show that

$$\sum_{n=1}^2 \frac{\mu_n}{k_n} \frac{\partial}{\partial k_n} \ln t_{nn}(k_1, k_2) = \frac{d}{dE} \left[ \frac{1}{\pi} \int_{\sigma_1}^{\infty} d\lambda \frac{\delta_1(\lambda) + \delta_2(\lambda)}{\lambda - E} \right], \quad (\text{A13})$$

the imaginary part of above relation therefore yields the relation in Eq.(A12).

For the trapped systems, if the integrated correlation function for each individual channel is defined by

$$C_n(t) = i \int_{-\infty}^{\infty} \frac{d\lambda}{2\pi} \left[ \int dr G_{nn}^{(trap)}(r, r; \lambda + i0) \right] e^{-i\lambda t}, \quad (\text{A14})$$

using Eq.(A11), we find

$$C_n(t) - C_n^{(0)}(t) \xrightarrow{\text{trap} \rightarrow \infty} \frac{it}{\pi} \int_{\sigma_n}^{\infty} \Delta_n(\epsilon) e^{-i\epsilon t} d\epsilon. \quad (\text{A15})$$

The inelastic effect for the single channel is embedded in the  $\Delta_n(E)$  functions, which is related to both phase shifts and inelasticity through Eq.(A7) and Eq.(A6).

Using the contact interaction model discussed in Sec. III C as a specific example, we can also show that

$$\begin{aligned} & \int_{-\infty}^{\infty} dr \left[ G_{nn}^{(\infty)}(r, r; E) - G_n^{(\infty,0)}(0; E) \right] \\ &= i \frac{\mu_n^2}{k_n^3} T_{nn} = \frac{\mu_n}{k_n^2} \frac{\eta e^{2i\delta_n} - 1}{2}, \end{aligned} \quad (\text{A16})$$

where the analytic expression of  $T_{nn}$ 's are given in Eq.(52), therefore

$$\frac{\mu_n}{k_n} \frac{\partial \Phi_n(E)}{\partial k_n} = -\text{Re} \left[ \frac{\mu_n^2}{k_n^3} T_{nn} \right] = -\frac{\mu_n}{k_n^2} \frac{\eta \sin(2\delta_n)}{2}, \quad (\text{A17})$$

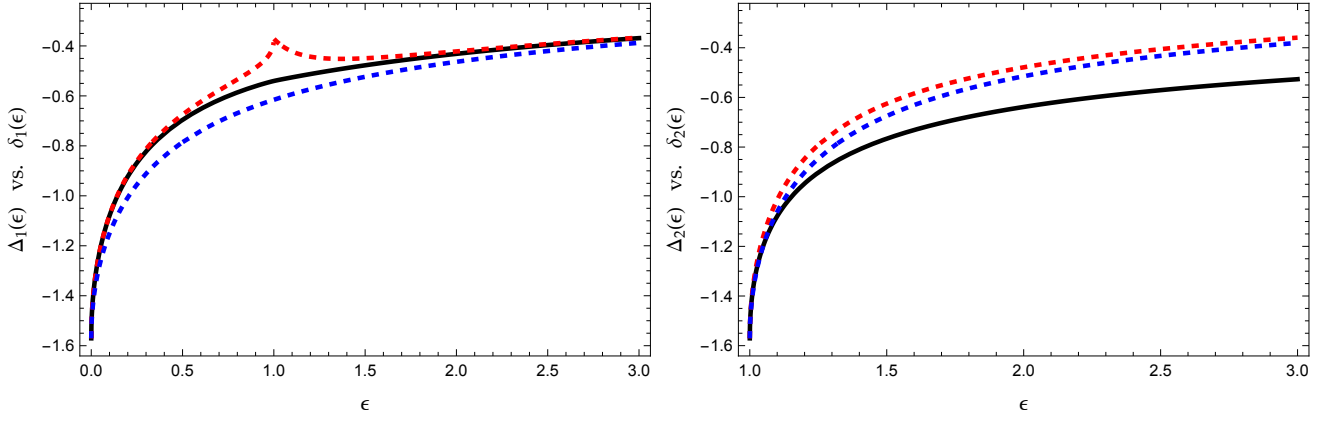


FIG. 6: Comparison of phase shifts in channel 1 (left) and channel 2 (right). The three curves correspond to:  $\Delta_n(\epsilon)$  (solid black),  $\delta_n(\epsilon)$  (dashed red), and  $-\cot^{-1}\left(\frac{k_n}{\mu_n V_n}\right)$  (dashed blue). The parameters are taken as:  $V_1 = 1.0$ ,  $V_2 = 0.8$ ,  $\gamma = 0.6$ ,  $\sigma_1 = 0$ ,  $\sigma_2 = 1$  and  $\mu_1 = \mu_2 = 1$ .

and  $\Delta_n(E)$  can be computed by

$$\Delta_n(E) = \delta_n(\sigma_n) - \int_{\sigma_n}^E d\lambda \frac{\mu_n}{k_n^2(\lambda)} \frac{\eta(\lambda) \sin(2\delta_n(\lambda))}{2}. \quad (\text{A18})$$

As  $\gamma \rightarrow 0$ , the two channels are completely decoupled,

leading to,

$$\Delta_n(E) \xrightarrow{\gamma \rightarrow 0} \delta_n(E) \rightarrow -\cot^{-1}\left(\frac{k_n}{\mu_n V_n}\right), \quad (\text{A19})$$

in each channel. The comparison of  $\Delta_n(E)$  vs.  $\delta_n(E)$  vs.  $-\cot^{-1}\left(\frac{k_n}{\mu_n V_n}\right)$  is demonstrated in Fig. 6. Significant effects of inelasticity can be observed in both channels as the difference between the solid and dashed curves.